LA-UR-02-6730

Approved for public release;
distribution is unlimited.

Title: Ion Dynamics in Helicon Sources

Author(s): John L. Kline, Matthew Balkey, paul Keiter, E. E. Scime, A. M. Keesee, X. Sun, R. F. Boivin, M. W. Zintl

Submitted to: 44th American Physical Society - Division of Plasma Physics Annual Meeting

Ion Dynamics in Helicon Sources

J. L. Kline, M. M. Balkey and P. A. Keiter
Los Alamos National Laboratory, Los Alamos, NM, 87545

E. E. Scime, A. M. Keesee, X. Sun, R Harding, and C Compton
Physics Department, West Virginia University, Morgantown, WV, 26505

R. F. Boivin
Physics Department, Auburn University, Auburn, AL, 36849

M. W. Zintl
Scientific Applications & Research Associates Inc., Huntington Beach, CA 92649

Recent experiments have demonstrated that ion dominated phenomena, such as the lower hybrid resonance, can play an important role in helicon source operation. In this work, we review recent ion heating measurements and the role of the slow wave in heating ions at the edge of helicon sources. We also discuss the relationship between parametrically driven waves and ion heating near the rf antenna in helicon sources. Recent measurements of parallel and rotational ion flows in helicon sources have important implications for particle confinement, instability growth, and helicon source operation. In this work we present new measurements of ion flows and summarize the important features of the flows.

I. Introduction

The first helicon source was built as a basic plasma research tool to investigate the left handed circularly polarized, whistler, wave in magnetized plasmas.[1] Although, the left handed, circularly polarized wave was not observed, those initial experiments demonstrated that the helicon source generated relatively high densities for laboratory plasmas, $n \sim 10^{12}$ cm^{-3}, with a large ionization fraction. Except for a few magnetoplasma experiments,[2,3] little interest was shown in the helicon source until the mid 80's, when silicon chip manufacturing began to grow rapidly. The relatively high densities and large ionization fraction for moderate input powers made the helicon source a good candidate for an advanced plasma-processing source. The primary goal of experiments on helicon sources until the late 90's was optimization for plasma processing.

Since the late 90's, helicon sources have been used as plasma sources for research in many areas of plasma physics including: space relevant high beta studies,[4] plasma propulsion,[5] and basic plasma science.[6,7] One problem associated with employing helicon sources in many of these research areas is that the essential physics of helicon sources has been poorly understood until only recently. Initial theoretical investigations of helicon sources focused on the excitation of bounded whistler, helicon, waves and the dynamics of electrons in those waves.[8,9] Later theoretical studies included the effects of the slower root to the cold plasma dispersion relation in a bounded cylinder, the so-called Trivelpiece-Gould mode.[10-12] Helicon waves are the faster phase velocity solution to the cold plasma dispersion relation.

Although the early experiments were performed at RF frequencies near the lower hybrid frequency (a frequency that is routinely used to heat ions) and later experiments indicated that ion dynamics near the lower hybrid frequency (define lower hybrid frequency here please) could play an important role in helicon sources,[13] ion dynamics in helicon sources has been largely ignored in theoretical studies. Ions are routinely assumed to be cold (less than 0.1 eV),[14] to flow out the end of linear helicon sources at the sound speed, and to have no significant rotational flow.[15] In this paper, we summarize a series of experiments that have examined ion heating and ion flows in the West Virginia University helicon source. The experimental apparatus is described in Section II. Ion heating observations and their relationship to slow wave resonances and parametrically driven waves are reviewed in Section III. Recent ion flow measurements are described in Section IV. Implications of the experimental measurements are discussed in Section V. Because of length limitations, we have not attempted to thoroughly reference the entire body of helicon source literature in this work. The reader is referred to references by Boswell and Chen[16,17] as they include extensive helicon source research bibliographies.

II. Experimental Apparatus

Ion dynamics experiments have been performed using two different helicon source plasma chambers on the Hot hELicon eXperiment (HELIX) at West Virginia University. The first chamber, HELIXa (Figure 1a), was a Pyrex™ tube that was 157 cm

long and 15 cm in diameter.[13] The all glass tube had a single set of four 2 ¾" Conflat™ crossing ports 57 cm from the front edge of the antenna. The second chamber, HELIXb (Figure 1b), was a hybrid chamber consisting of a 60 cm long, 10 cm diameter Pyrex™ section connected to a 100 cm long, 15 cm diameter stainless steel section.[18] The stainless steel section had one set of four 6" Conflat™ crossing ports and four sets of four 2 ¾" Conflat™ crossing ports. The 2 ¾" Conflat™ crossing ports are spaced evenly on either side of the four 6" crossing ports. The other end of the stainless steel chamber was connected to a large 2 m diameter, 4 m long space simulations chamber (LEIA).[4] The other end of the glass section of the chamber was connected to a 540 l/s turbomolecular drag pumping station. Fill gas was added through an inlet on the stainless steel flange connecting the glass section of the chamber to the pumping station. A 19 cm, $m = +1$ helical antenna with an ENI 30 db, 2 kW amplifier was used to generate an argon plasma for all experiments described in the present paper.

Both chambers were surrounded by the same set of ten electromagnets connected in series providing an axial magnetic field of 400 - 1185 Gauss with the magnetic field. For all the experiments described here, the LEIA magnetic field was fixed at 36 Gauss. HELIXb was operated in two different magnetic field configurations, a ten-magnet coil configuration and an eight-magnet coil configuration. In the eight-coil configuration, the last two electromagnets between HELIXb and LEIA were disconnected. Removing the two coils allowed the eight coil configuration to reach magnetic fields of 1300 Gauss.[18] However, in the eight-coil configuration, the outer magnetic field lines ($r > 3.5$ cm) intersect the wall of the stainless steel chamber near the junction with the LEIA chamber thereby imposing a partially conductive axial boundary. Because HELIXa was connected to LEIA via a 6" stainless steel bellows, while the stainless steel chamber of HELIXb was directly connected to LEIA, the additional distance between HELIXa and LEIA also resulted in outer magnetic field lines intersecting conductive bellows walls. Therefore, the axial boundary conditions in the HELIXa and eight-coil HELIXb experiments were somewhat similar. With HELIXb in the ten-coil configuration, nearly all the magnetic field lines terminated on the inner walls of the LEIA.

Electron temperatures and densities were measured with an rf compensated Langmuir probe.[19] Density measurements were confirmed on a subset of plasma

parameters with a steady state microwave.[20] Ion temperatures and flows, both parallel and perpendicular to the applied magnetic field, were obtained from direct measurements of the ion velocity space distribution by laser induced fluorescence (LIF).[21,22] In HELIXa, the LIF measurements could only be measured at a single axial point 57 cm from the front edge of the antennal in both perpendicular and parallel directions.[23] In HELIXb, the LIF measurements were performed at the axial positions labeled A, B, and C in Figure 1b, where position A was 5 cm, position B was 35 cm, and position C was 66 cm from the front of the antenna. At position C, LIF measurements could be made over a 2 dimensional cross of the plasma column. Details of the LIF system for HELIXa and HELIXb have been published elsewhere.[13,18] The electrostatic fluctuation measurements were made with a fixed pair of probes at axial position "B". The electrostatic probe consisted of two Langmuir probe tips separated by 5.8 mm. So that high frequency floating potential fluctuations could be measured, the electrostatic probe tips were not rf compensated.

III. Heating in Helicon Plasmas

Several key characteristics of ion heating have been observed in helicon plasmas: anisotropic ion temperatures that peak at particular values of applied magnetic field and rf frequency, an axial ion temperature profile peaked downstream from the antenna, and an inverse relationship between ion temperature.

IIIa. Characteristics of the Ion Temperatures in HELIX

Anisotropic ion temperatures measured in HELIXa were completed unexpected given the large ion-ion collision frequencies in dense helicon plasmas. That energy is coupled into the ions in a preferential direction provides a critical clue as to the origin of ion heating in helicon sources. Our initial study of the ion temperatures demonstrated that the ion temperature anisotropy scaled linearly with the magnetic field strength.[23] The perpendicular ion temperature increases linearly with magnetic field while the parallel ion temperatures remain about the same. Perpendicular and parallel ion temperatures verses magnetic field strength in HELIXa (from Scime *et al.*[23]) along with measurements in HELIXb in the ten coil configuration are shown in Figure 2. Although the helicon

source operating parameters were different for the different chambers, ion temperature anisotropy was evident in both sets of measurements. Only at the highest magnetic field strengths did the perpendicular temperatures differ.

Ion temperature measurements in HELIXb in the eight-coil configuration were remarkably different.[24] Figure 3 shows both perpendicular and parallel ion temperatures measured on axis at position "B" (35 cm position) in HELIXb at two different driving frequencies with all other parameters the same. At 9 MHz, the ion temperatures increased with increasing magnetic field strength and there was no significant ion temperature anisotropy. At 13.5 MHz, a small temperature anisotropy existed at low magnetic field strengths but disappeared as the magnetic field strength was increased. The perpendicular ion temperatures peaked at a specific value of magnetic field strength and then decreased as the magnetic field increased further. The dependence of the ion temperature on the magnetic field strength was clearly different for the two rf driving frequencies even though the rf frequency was hundreds of times greater than the ion cyclotron frequency.

Figure 4 shows the perpendicular and parallel ion temperatures at an rf frequency of 9 MHz and a magnetic field strength of 1185 G. Although the ion temperature was isotropic at the center of the plasma, the ion temperature was anisotropic at the plasma edge where the perpendicular ion temperature increased and the parallel ion temperature decreased. A flat or peaked at the edge perpendicular ion temperature profile could only result from either edge ion heating or a large axial thermal conductivity. As will be shown later, there is strong axial gradient in the perpendicular ion temperature profile. Therefore, these measurements demonstrated that the ions were heated at the edge of helicon sources and preferentially in the perpendicular direction.

The combined stainless steel and glass HELIXb vacuum chamber was specifically designed to permit ion temperature measurements at four different axial locations: -24 cm, 5 cm (position A), 35 cm (position B), and 60 cm (position C) from the front edge of the antenna. Perpendicular ion temperatures in HELIXb in the ten-coil configuration at these four axial locations are shown in Figure 7 for two different magnetic field strengths. At magnetic field strengths less than approximately 500 Gauss, the ion temperature decreases monotonically with increasing distance from the antenna ($z > 0$). At magnetic

field strengths greater than approximately 500 Gauss, the perpendicular ion temperatures peak downstream from the antenna ($z \sim 35$ cm). The downstream ion temperature peak at higher magnetic field strengths corresponds to the slow wave correlated ion heating discussed previously. Previous reports of increased electron densities downstream of the helicon antenna have been attributed to simple pressure balance[25] or parametrically driven ion sound instabilities.[26,27] Note that the ion temperatures on the backside of the antenna are lower than those in the front of the antenna in both cases, confirming a preferential direction for the energy deposition into the ions. The perpendicular ion temperatures also peak downstream from the antenna in HELIXb in the eight coil configuration.[24] Also note that near the antenna, the perpendicular ion temperatures still exceed what would be expected for simple collisional equilibration with the much hotter electrons.[13] Since the ion heating near the antenna was not consistent with ion damping of slow waves, other ion heating mechanisms, such ion heating due to parametric sound turbulence were considered.[26,27]

IIIb. Slow Wave Ion Heating

The mechanism for the edge perpendicular ion heating was identified by careful investigation of the magnetic field strength and rf frequency dependence of the ion heating. The first detailed measurements of the ion temperatures over a large range of rf driving frequencies and magnetic field strengths by Balkey *et al.*[13] showed that the perpendicular ion temperatures were correlated with the lower hybrid frequency, but peaked at values about 70% below the lower hybrid frequency (Figure 5a). After the Balkey *et al.*[13] experiments were performed in HELIXa, similar experiments were performed with HELIXb in the eight coil configuration at location "B" (Figure5b).[18,24] The perpendicular ion were again correlated with and peaked below the on axis lower hybrid frequency. However, the wider magnetic field an rf frequency ranges attained in the HELIXb experiments showed a localized peak in perpendicular ion temperature at a specific set of magnetic field and rf frequency values.

The cold plasma dispersion relationship has two solutions as the driving frequency approaches the lower hybrid frequency: the fast, "helicon", wave and the slow, "Trivelpiece-Gould" mode, wave. Near the lower hybrid frequency, the perpendicular

wave number for the slow wave undergoes a resonance while the perpendicular wave number for the helicon wave continues smoothly through the lower hybrid frequency.[28] The resonance in the perpendicular wave number of the slow wave can reduce the phase speed in the perpendicular direction to speeds that are close enough to the ion thermal speed such that ion Landau damping can occur.[18] The result is an ion heating mechanism with a preferential direction with respect to the applied magnetic field.

The theoretically predicted characteristics of the slow wave are consistent with the measured ion temperatures. First, the radial profile of both the perpendicular and parallel ion temperatures shown in Figure 4 indicates that the largest anisotropic ion heating occurs near the edge of the plasma. Theory predicts that slow waves are primarily surface waves in helicon sources because they are strongly damped as the plasma density increases towards the center of a helicon source discharge.[12] Second, the decrease in lower hybrid frequency towards the edge of the plasma (due to density profile effects) results in a peak in the perpendicular wave number of the slow wave for a specific range of magnetic field strength and rf frequencies.[18,24] Figure 6a shows the ion temperatures measured in HELIXb at the z = 35 cm location in the eight-coil configuration. The solid white line is along the on-axis lower hybrid frequency for a fixed peak density of 2×10^{12} cm^{-3} while the dashed line represents the lower hybrid frequency at the plasma edge for a fixed density of 1×10^{11} cm^{-3}. Although the densities vary with magnetic field strength, these values include the range of peak and edge densities for magnetic field strengths above 700 Gauss. Using the cold plasma dispersion relationship of Cho including ion terms and collisions,[28] the magnitude of the perpendicular wave numbers in HELIXb as a function of magnetic field strength, rf frequency, and plasma radius can be calculated using a series of simple homogeneous annuli with different plasma densities.[18] For each rf frequency and magnetic field strength, the perpendicular wave numbers were calculated at different radial positions using a parabolic density profile. The largest value of the perpendicular wave number across the plasma radius was recorded and plotted as a function of rf frequency and magnetic field strength (Figure 6b). The peak values for the normalized wave numbers occur at the same values of rf frequency and magnetic field strength as the peak perpendicular ion temperatures. Thus, the evidence of edge perpendicular ion heating and the rf and magnetic field strength

dependencies of the ion heating are consistent with the conclusion that ion damping of slow waves in the edge of helicon sources is responsible for ion heating in helicon source. In fact, except for high frequency axial current measurements of Blackwell and Chen,[29] these ion heating measurements are the only other experimental evidence that slow waves truly exist in helicon sources.[24] Direct measurements of such short wavelength waves, $\lambda < 1$ mm, are still beyond the capabilities of conventional helicon source diagnostics. We note, however, that recent microwave scattering experiments are close to being able to directly measure short wavelength fluctuations in helicon sources.[24,30]

IIIc. Ion Heating Via Parametric Decay of the Helicon Wave

Electrostatic, parametrically driven instabilities have been observed in the HELIXb experiments.[31] Figure 8 shows the electric field power spectrum at position "B" in HELIXb in the eight-coil configuration. The 11 MHz pump wave, the forward and backward propagating waves (stokes and anti-stokes), and a low frequency mode, beat, wave are evident in the power spectrum. A fifth spectral peak around 9 MHz is an experimental artifact and exists in all of our electrostatic power spectrum measurements. The power spectrum shows that the frequency matching condition, $f_2 = f_1 \pm f_o$, i.e., energy conservation is satisfied. Measurements of the wave numbers and magnetic field fluctuation power spectra confirm that the wave number matching condition, i.e, momentum conservation, is also satisfied and that the parametrically excited waves are purely electrostatic.[31] Radial measurements of the wave amplitudes show that the electrostatic waves are localized to the center of the plasma ($r < 3$ cm). The experimental evidence, including wave phase velocity and propagation direction measurements, are consistent with the interpretation that the parametrically excited waves (the sidebands) are electrostatic lower hybrid waves and the low frequency mode is an ion acoustic wave. The measured phase speeds of the electrostatic lower hybrid waves are too large for significant interaction with ions. However, the phase speed of low frequency wave is on the order of three times the ion thermal velocity and ion damping of such waves is theoretically possible.

A comparison of the perpendicular ion temperatures at position "A" (near the antenna) with the spectral amplitude of the low frequency wave as measured with the

electrostatic probe is shown in Figure 9 as a function of magnetic field strength and rf driving frequency. There is a rough correlation between the measured perpendicular ion temperatures and the amplitude of the low frequency waves. The wave numbers of the low frequency waves are larger at lower rf driving frequencies where the fluctuation amplitudes peak up.[31] The larger wave numbers result in wave phase speeds within a factor of 2.5 of the ion thermal velocity. These measurements demonstrate that electrostatic waves are parametrically excited in HELIXb and that amplitude of the low frequency beat wave is largest (and the phase speeds smallest) for the same parameters are which the perpendicular ion temperatures near the rf antenna are largest.

IV. Ion Flow Measurements

Ion heating is not the only dynamic ion process that is important to understanding operational details in helicon sources. Plasmas typically flow along the magnetic field at the sound speed. The more mobile electrons try to leave the system but are held back by an ambipolar electric field setup between the electrons and ion. The ions' inertia sets the sound speed that is inversely proportional to the ion mass. However, ion flow measurements in argon plasmas show that the ions flow along the magnetic field near the ion thermal velocity, which is about ten time less than the sound speed. Measurements of the azimuthal ion velocities have shown that the plasma rotates as a solid body. This rotation could lead to Kelvin-Helmholtz instabilities due to azimuthal velocity shear at the edge of the plasma. Parallel and azimuthal flow measurements will be discussed in this section.

IV a. Axial Flows

In the past decade, a number of helicon sources have been constructed to investigate the possibility of using helicon sources as plasma thrusters.[5,32] At WVU, an interest in instabilities driven by shear in the parallel flow [33-37] has motivated a series of experiments designed to investigate parallel flows in and exiting from helicon sources. The parallel velocities of argon ions, and helium neutrals, in the WVU helicon source were determined by direct LIF measurements of the parallel ion distribution functions.

Measurements of argon ion flow along the magnetic field inside the HELIXa chamber towards the LEIA chamber are shown in Figure 10a as a function of neutral pressure. Parallel flow normalized to the parallel ion temperature as a function of magnetic field strength is shown in Figure 10b for HELIXb in the ten-coil configuration. In both cases, the largest parallel flows inside the helicon source chamber are slightly larger than the parallel ion thermal speed, but considerably smaller than the ion sound speed ($C_s = (V_{te}/m_i)^{1/2}$). Less accurate measurements of parallel flow by Light *et al.* using a mach probe produce similar results.[15] Thus, contrary to typical assumptions, ions flow out the end of helicon sources at the ion thermal speed. The parallel ion flow profile is not uniform across the plasma diameter and flows maximized on axis and maximized at the plasma edge have both been observed in HELIXb.[38] The shear in the parallel flow normalized to the ion gyrofrequency can be as large as $(dV/dx)(1/\Omega_i) \sim \pm 0.5$, sufficiently large to drive both shear modified ion acoustic waves and shear modified ion cyclotron waves in thermally anisotropic.[33-37]

What happens to the parallel ion flow as the magnetic field lines diverge into the expansion chamber is not well understood. Measurements in LEIA 1 m from the end of the helicon source find little to no evidence of parallel ion flow in argon plasmas. However, recent parallel flow experiments (using LIF on argon ions) found high-speed flows, on the order of 10,000 m/s, emanating from a small aperture at the end of the MNX helicon source.[39] The aperture separates the high-power MNX helicon source from a larger expansion region with an expanding magnetic field geometry. If neutral braking, due to charge-exchange collisions, was responsible for the slowing of the parallel flow in the HELIX-LEIA experiments, a net flow in the neutral atoms might be expected. Yet measurements of neutral helium atoms (with LIF) also found no net flow in the region directly downstream from the HELIXa chamber during helium plasma operation. The dynamics of the ions (and neutrals) in the expansion region are the subject of a series of ongoing experiments at WVU using LIF probes that can scan along the plasma axis.

IV b. Rotational Flows

Another important ion dynamics issue concerns rotational flow in helicon sources. In recent studies of the saturation of plasma density with increasing magnetic field in

helicon sources Light *et al.*[15] proposed that enhanced diffusion to the excitation of resistive drift waves could explain the plasma poor confinement in helicon sources at high magnetic field strengths. Those studies ignored other potential instabilities, such as the Kelvin-Helmholtz instability, because there was no experimental evidence of plasma rotation in helicon sources. Measurements of the total perpendicular ion velocity in argon HELIXb plasmas are shown in Figure 11 as a function of position in a cross-sectional plane for HELIXb in the ten-coil configuration. The flow vectors were measured by combining LIF measurements made along the vertical and horizontal directions at roughly 100 locations across a cross section of the plasma at location A (see Figure 1). The flow vectors overlay a contour plot of metastable ion density, roughly proportional to the square of the plasma density. The ions clearly rotate around the central density peak. Therefore, ion flows could play an important role in exciting instabilities that could degrade plasma confinement, e.g., flow driven Kelvin-Helmholtz instabilities.

V. Discussion

When ion temperatures are large in helicon sources, $T_i > 0.75$ eV, the ions can store a significant fraction of the kinetic energy in the source, assuming $T_e \sim 4$ eV. Therefore, understanding how rf energy is ends up in the ions is critically important to understanding power balance in helicon sources As ion temperatures increase, the ion gyroradius increases and in plasmas with small ionization fractions dominated by ion-neutral collisions, ion confinement times should correspondingly decrease. Since higher diffusion rates require more input power to maintain plasma densities, helicon source power balance calculations should also include the effects of neutral-collision driven transport.

The experimental measurements reported here have demonstrated that: the ions are preferentially heated in the perpendicular direction; ion heating is maximum at some finite distance downstream from the antenna; and that the largest amount of ion heating downstream of the rf antenna occurs when the rf frequency matches the local lower hybrid frequency at the edge of the plasma. Comparison of the measurements with theoretical calculations strongly suggests that ion damping of slow waves is responsible for the observed ion heating downstream of the antenna. Close to the rf antenna,

additional ion heating mechanisms appear to be important. Ion damping of parametrically driven waves is one possible mechanism that could provide for the observed ion heating and there is some correlation between the observed ion heating and the amplitudes of the parametrically driven waves in the helicon source.

Preferential ion diffusion can also lead to the establishment of radial electric fields and thereby induce plasma rotation in helicon sources. The recent ion rotation measurements in HELIXb clearly show ion rotation and such rotational flows must be considered in analysis of the observed low frequency instabilities in helicon sources. Parallel flow measurements indicate that ions flow out of the open end of helicon sources at roughly the parallel ion thermal speed, not at the ion sound speed.

Altogether, the ion dynamics in helicon sources cannot be ignored. Typical assumptions that the ions are cold (approximately room temperature) or that the axial plasma flows are near the plasma sound speed have been shown to be untrue for a small subset of the typical helicon operating parameters. Therefore, theoretical predictions should carefully consider the role of the ions in helicon plasmas. Furthermore, the role of the ions should be considered when choosing the helicon source for a specific application.

Acknowledgments. Work at WVU was performed with support from National Science Foundation grant ATM-99988450 and the U.S. Department of Energy under grant DE-FG02-97ER54420. We would like to thank the members of the WVU machine shop, Doug Mathess, Tom Milan, and Carl Weber, for all of their efforts contributing to the work done by the WVU Helicon group. We also acknowledge David Montgomery of Los Alamos National Laboratory and Vladimir Mikhailenko of Kharkov National University for useful discussions on the subjects of parametric decay and ion heating.

References

[1]Boswell, R.W., Phys. Lett. A, **33** 457 (1970).
[2]Boswell, R.W., Phys. Lett. A, **55A** 93 (1975).
[3]Boswell, R.W., Nature, **258** 58 (1975).
[4]Keiter, P.A., Scime, E.E., Balkey, M.M., Boivin, R., Kline, J.L., and Gary, S.P., Phys. Plasmas, **7** 779 (2000).
[5]Chang Diaz, F.R., Goulding, R.H., Bengtson, R.D., Wally Baity, F., Sparks, D., Bussell, R.G., Jr., Barber, G.C., McCaskill, G., Jacobson, V.T., Carter, M.D., Ilin, A.V., and Glover, T.W., Fusion Technology, **35** 243 (1999).
[6]Hanna, J. and Watts, C., Phys. Plasmas, **8** 4251 (2001).
[7]Franck, C.M., Grulke, O., and Klinger, T., Phys. Plasmas, **9** 3254
[8]Chen, F.F., Hsieh, M.J., and Light, M., Plasma Sources Sci. Techol., **3** 49 (1994).
[9]Blevin, H.A. and Christiansen, P.J., Austrailian Journal of Physics, **15** 501 (1966).
[10]Chen, F.F. and Arnush, D., Phys. Plasmas, **4** 3411 (1997).
[11]Borg, G.G. and Boswell, R.W., Phys. Plasmas, **5** 564 (1998).
[12]Shamrai, K.P. and Taranov, V.B., Phys. Lett. A, **204** 139 (1995).
[13]Balkey, M.M., Boivin, R.F., Kline, J.L., and Scime, E.E., Plasma Sources Science and Technology, **10** 284 (2001).
[14]Chen, F.F., Plasma Sources Science & Technology, 458 (1998).
[15]Light, M., Chen, F.F., and Colestock, P.L., Phys. Plasmas, **8** 4675 (2001).
[16]Chen, F.F. and Boswell, R.W., IEEE Transactions on Plasma Science, **25** 1245 (1997).
[17]Boswell, R.W. and Chen, F.F., IEEE Transactions on Plasma Science, **25** 1229 (1997).
[18]Kline, J.L., Scime, E.E., Boivin, R., Keesse, A., and Sun, X., Plasma Sources Science and Technology, **11** 413 (2002).
[19]Sudit, I.D. and Chen, F.F., Plasma Sources Sci. Techol., **3** 162 (1994).
[20]Scime, E.E., Balkey, M.M., Boivin, R., and Kline, J.L., Rev. Sci. Instrum., (2000).
[21]Hill, D.H., Fornaca, S., and Wickham, M.G., Rev. Sci. Instrum., **54** 309 (1983).
[22]Stern, R.A. and Johnson, J.A., III, Phys. Rev. Lett., **34** 1548 (1975).
[23]Scime, E.E., Keiter, P.A., Zintl, M.W., Balkey, M.M., Kline, J.L., and Koepke, M.E., Plasma Sources Sci. Techol., **7** 186 (1998).
[24]Kline, J.L., Scime, E.E., Boivin, R.F., Keesse, A., and Sun, X., Phys. Rev. Lett., **88** 195002 (2002).
[25]Sudit, I.D. and Chen, F.F., Plasma Sources Sci. Techol., **5** 43 (1996).
[26]Akhiezer, A.I., Mikhailenko, V.S., and Stepanov, K.N., Ukrayins'kyi Fizychnyi Zhurnal, **42** 990 (1997).
[27]Akhiezer, A.I., Mikhailenko, V.S., and Stepanov, K.N., Phys. Lett. A, **245** 117 (1998).
[28]Cho, S. and Kwak, J.G., Phys. Plasmas, **4** 4167 (1997).
[29]Blackwell, B.D. and Chen, F.F., Phys. Rev. Lett., (2002).
[30]Kaganskaya, N.M., Krämer, M., and Selenin, V.L., Phys. Plasmas, **8** 4694 (2001).
[31]Kline, J.L. and Scime, E.E., Phys. Plasmas, (2003).
[32]Cohen, S.A., Berlinger, B., Corso, V., Fahmy, F., Gorman, J., Levinton, F., Lemunyan, G., and Fredriksen, A., Bulletin of the American Physical Society, **44** (1999).
[33]Ganguli, G., Slinker, S., Gavrishchaka, V., and Scales, W., Phys. Plasmas, 2321 (2002).
[34]Gavrishchaka, V., Koepke, M.E., and Ganguli, G., Phys. Plasmas, 3091 (1996).
[35]Gavrishchaka, V.V., Ganguli, S.B., and Ganguli, G.I., Phys. Rev. Lett., 728 (1998).
[36]Spangler, R.S., Scime, E.E., and Ganguli, G.I., Phys. Plasmas, 2526 (2002).

[37]Scime, E.E., Keesee, A.M., Spangler, R.S., Koepke, M.E., Teodorescu, C., and Reynolds, E.W., Phys. Plasmas, **9** 4399 (2002).
[38]Sun, X., Boivin, R., Keesse, A., Kline, J., Scime, E., Spangler, R., and Woehrman, M., Bulletin of the American Physical Society, **46** 59 (2001).
[39]Cohen, S.A., (*Private Communication*) 2002.

Figure 1: a) A schematic diagram of HELIXa. b) A schematic diagram of HELIXb.

Figure 2: a) (◇) Perpendicular and (◆)parallel ion temperature measurements as a function of magnetic field strength in HELIXa for a fill pressure of 2 mTorr , a RF driving frequency of 9 MHz and an RF power of 400 Watts. b) (○) Perpendicular and (●) parallel ion temperature measurements as a function of magnetic field strength in HELIXb for a fill pressure of 6.7 mTorr , a RF driving frequency of 9 MHz and an RF power of 750 Watts.

Figure 3: a) On axis (○) perpendicular and (□) parallel ion temperature as a function of magnetic field strength for HELIXb in the eight coil configuration at position "B" with a fill pressure of 6.7 mTorr, and 750 Watts of rf power for a) a rf frequency of 9 MHz and b) a rf frequency of 13.5 MHz

Figure 4: a) (○) Perpendicular and (□) parallel ion temperatures versus radius for a fill pressure of 6.7 mTorr and a rf power of 750 Watt for an rf frequency of 9 MHz

Figure 5: a) Ion temperatures as a function of rf frequency and magnetic field strength in HELIXa. b) Ion temperatures as a function of rf frequency and magnetic field strength in HELIXb in the eight coil configuration at location "B". The white lines show the range parameters covered in the HELIXa experiments.

Figure 6: a) Calculated normalized wave numbers, $k_{\perp}v_{thi}/\omega$, from the cold plasma slow wave model. b) ion temperatures measured at position "B" with HELIXb in the eight coil configuration for a fill pressure of 6.7 mTorr and a rf power of 750 Watts. The solid white line represents the on axis lower hybrid frequency and the dashed line represents the edge lower hybrid frequency assuming plasma densities of 2×10^{12} cm^{-3} and 1×10^{11} cm^{-3} respectively.

Figure 7: Perpendicular ion temperatures at different axial locations for a magnetic field strength of (◆) 453 and (○) 808 Gauss.

Figure 8: Parametric decay spectrum for an rf frequency of 11 MHz and a magnetic field strength of 845 Gauss at location "B" in HELIXb in the eight coil configuration.

Figure 9: a) perpendicular ion temperatures at location "A" and b) signal amplitude of the low frequency wave at location "B" with HELIXb in the eight coil configuration for a fill pressure of 6.7 mTorr and a rf power of 750 Watts.

Figure 10: a) parallel plasma flows versus fill pressure and b) parallel plasma flows normalized to the ion thermal speed versus magnetic field strength for a fill pressure of 3.0 mTorr and a rf power of 750 Watt for an rf frequency of 9 MHz.

Figure 11: Ion metastable density and rotational flow measurements of a two dimensional plasma cross section in HELIX at position "C" for a fill pressure of 3.0 mTorr and a rf power of 750 Watt for an rf frequency of 9 MHz.

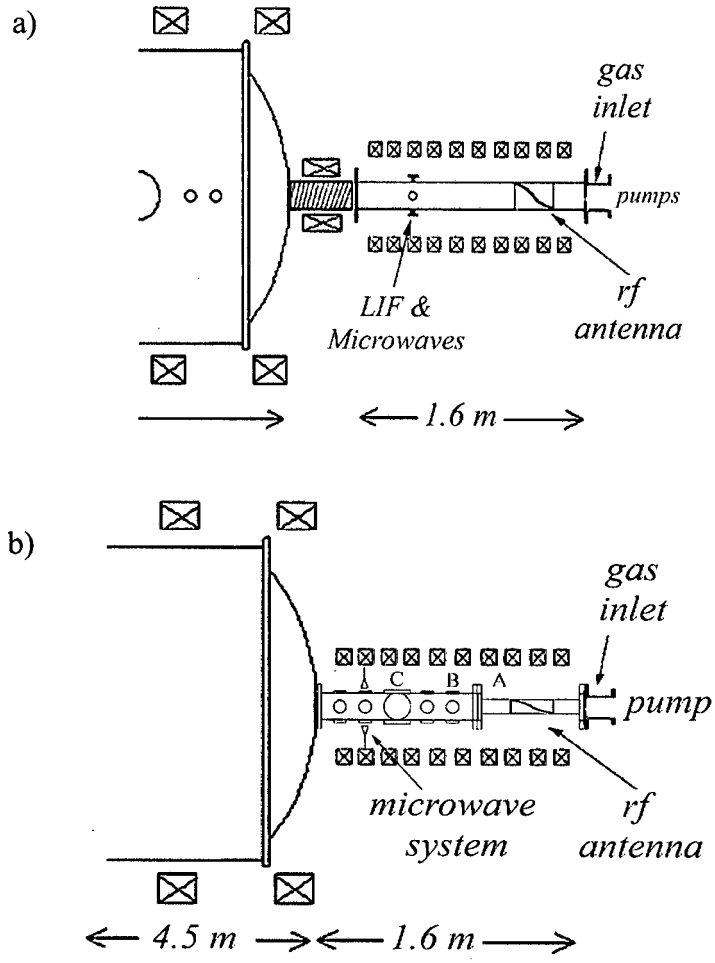

Figure 1, Kline *et al.*

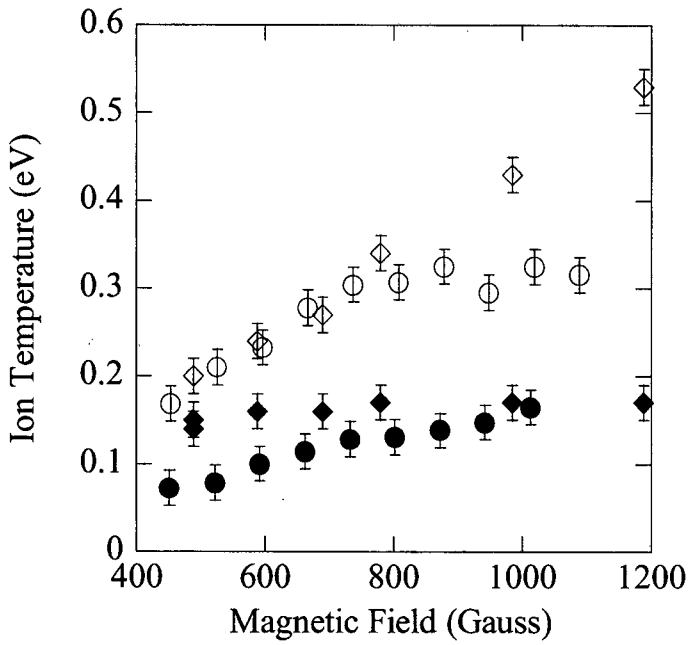

Figure 2, Kline *et al.*

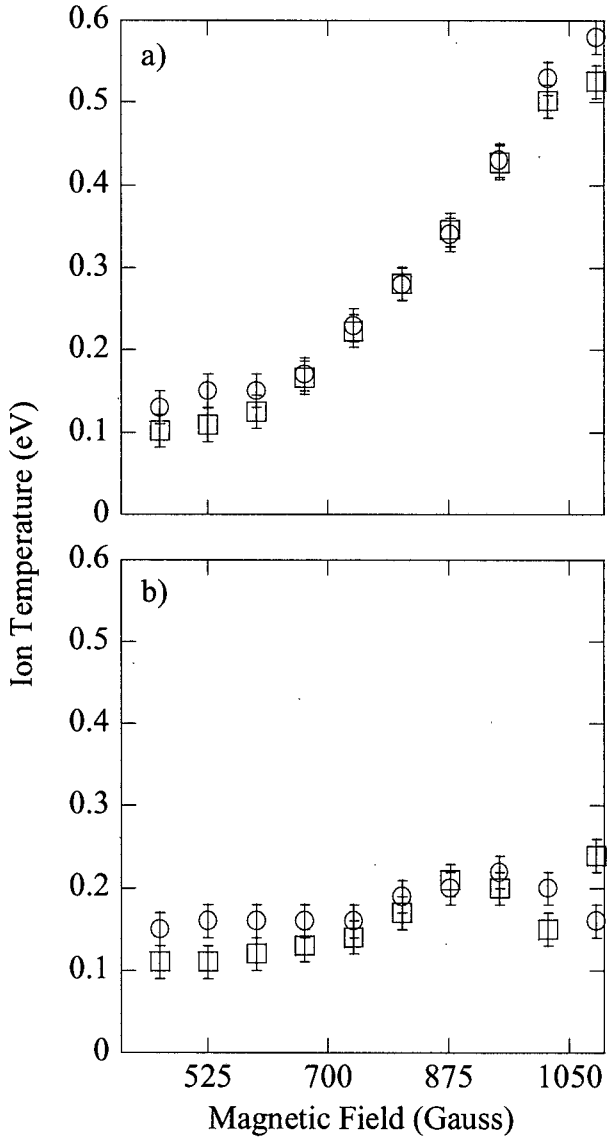

Figure 3, Kline *et al.*

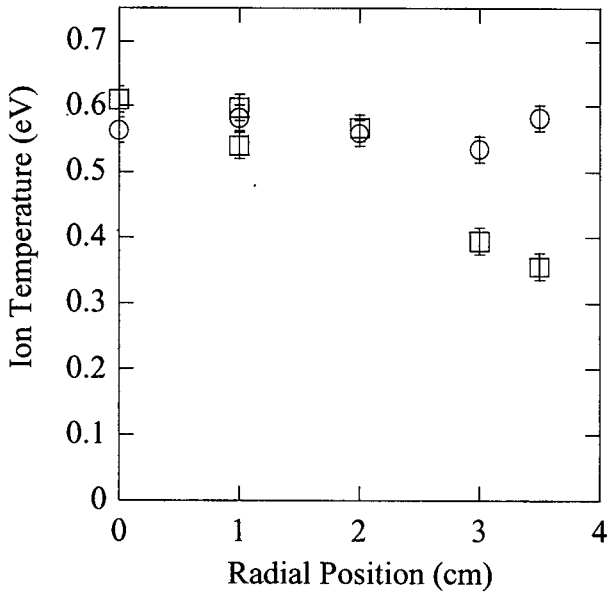

Figure 4, Kline *et al.*

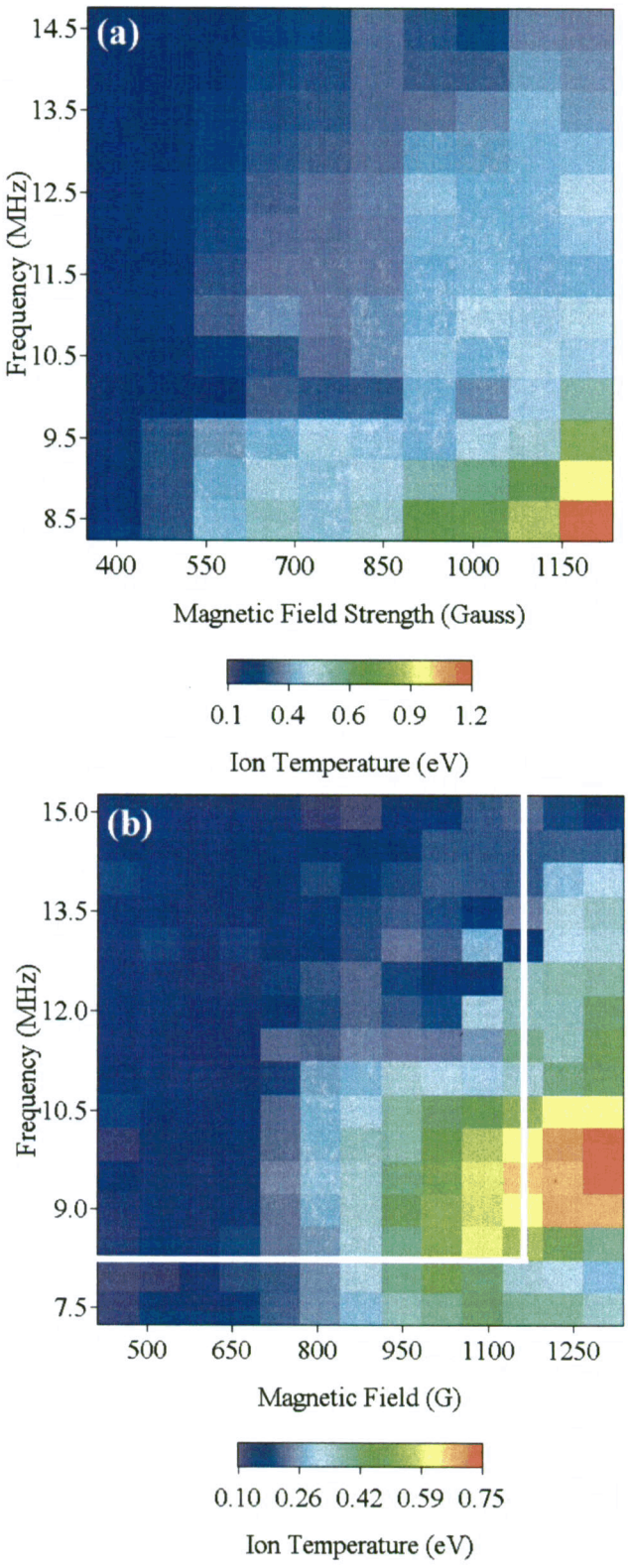

Figure 5, Kline *et al.*

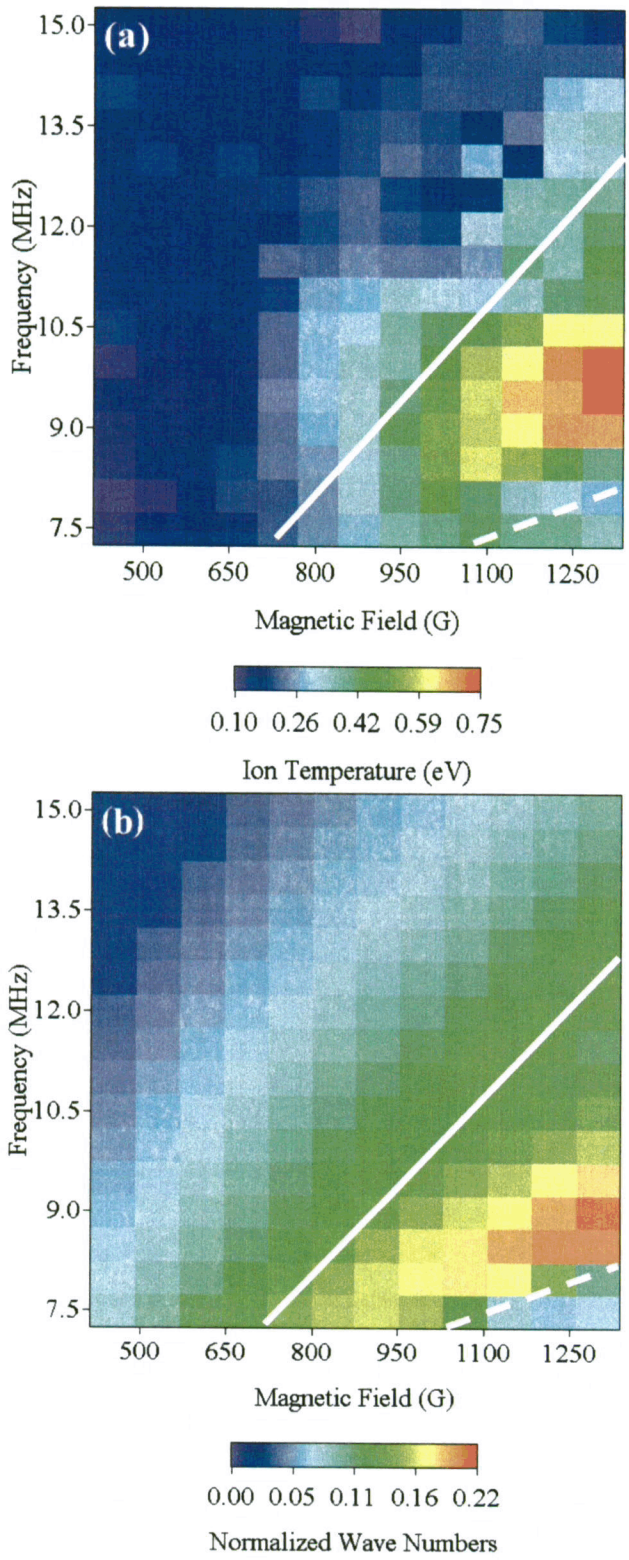

Figure 6, Kline *et al.*

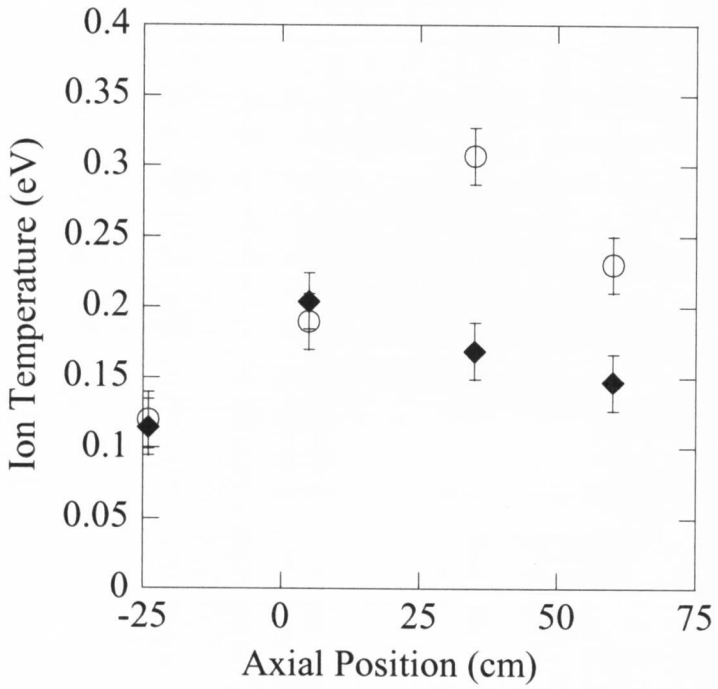

Figure 7, Kline *et al.*

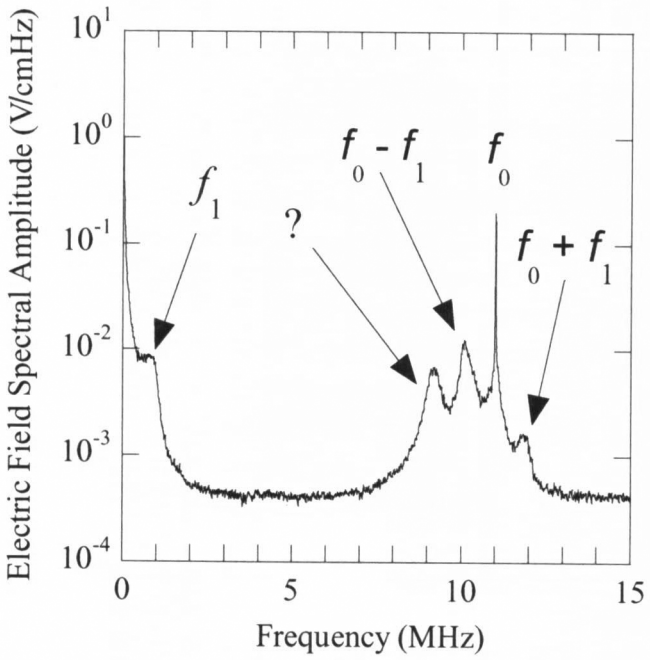

Figure 8, Kline *et al.*

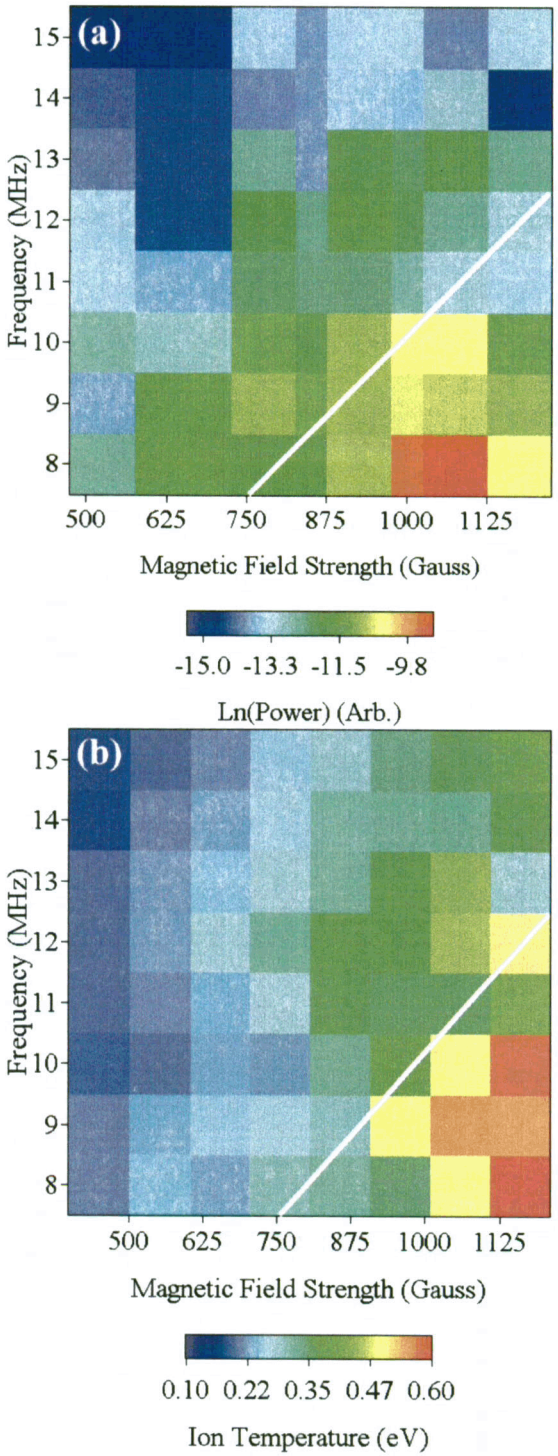

Figure 9, Kline *et al.*

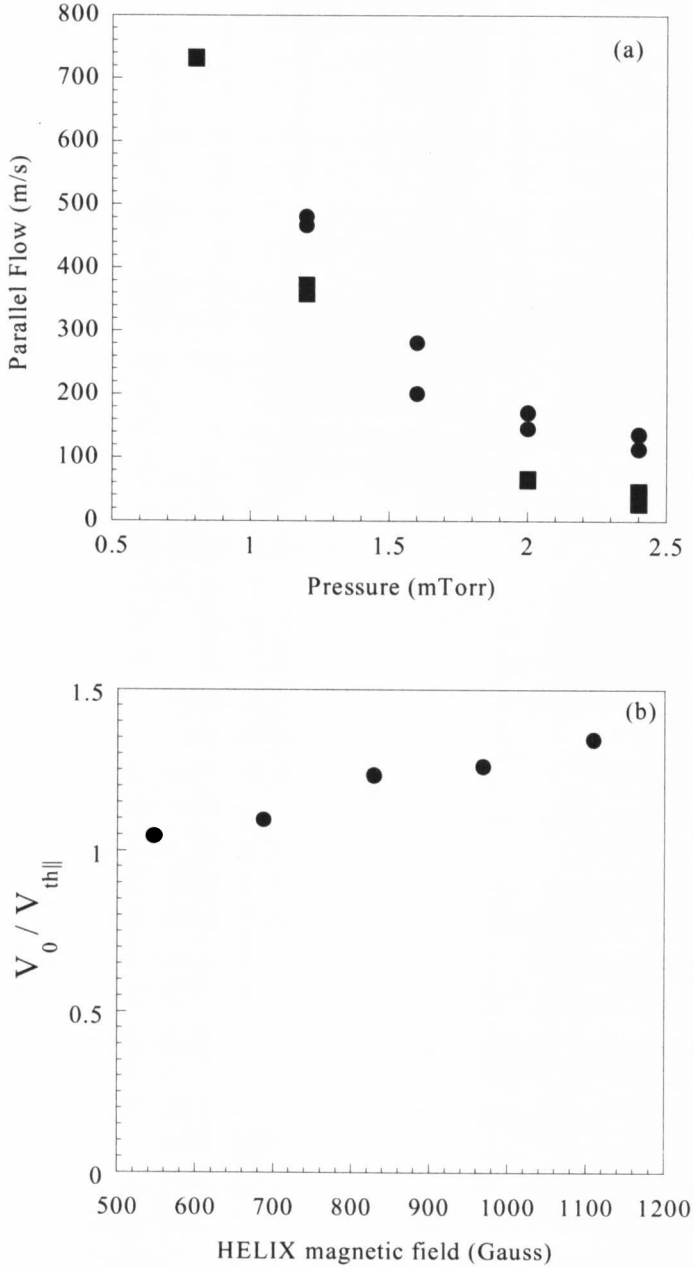

Figure 10, *Kline et al.*

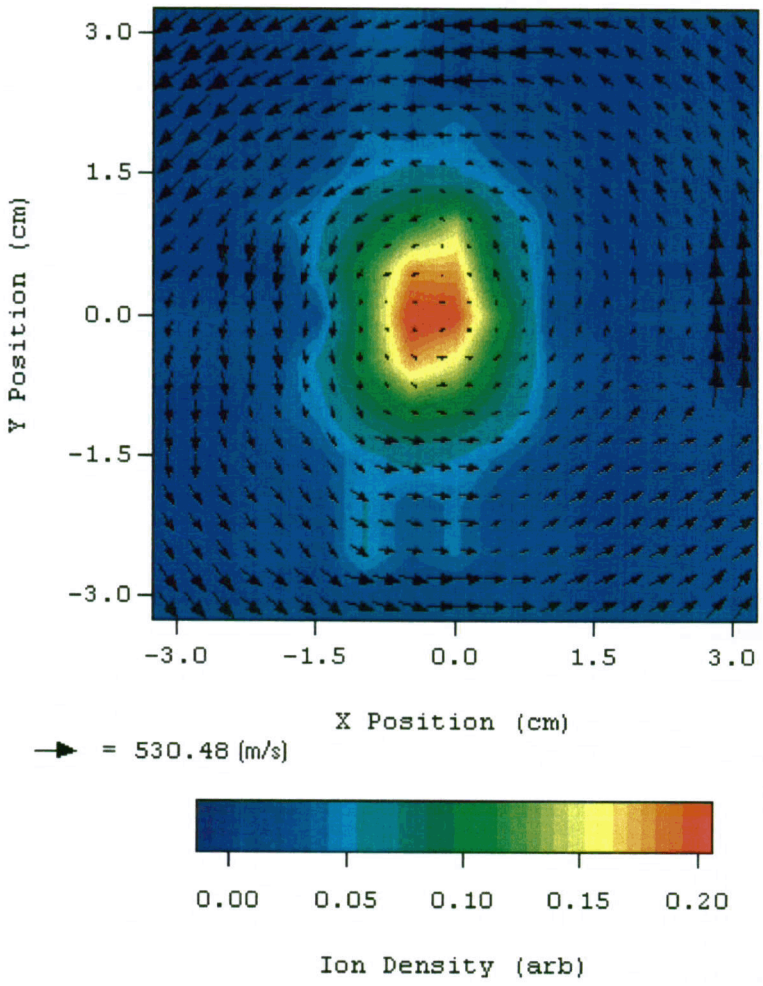

Figure 11, *Kline et al.*